Bioorganic & Medicinal Chemistry xxx (2014) xxx–xxx

Contents lists available at ScienceDirect

Bioorganic & Medicinal Chemistry

journal homepage: www.elsevier.com/locate/bmc

Synthesis and biological evaluation of podophyllotoxin congeners as tubulin polymerization inhibitors

Ahmed Kamal [a,d,*], T. Srinivasa Reddy [a,b], Sowjanya Polepalli [c], Nekkanti Shalini [d], V. Ganga Reddy [a], A. V. Subba Rao [a], Nishant Jain [c], Nagula Shankaraiah [d]

[a] Medicinal Chemistry and Pharmacology, CSIR-Indian Institute of Chemical Technology, Hyderabad 500 007, India
[b] IICT-RMIT Research Centre, CSIR-Indian Institute of Chemical Technology, Hyderabad 500 007, India
[c] Chemical Biology, CSIR-Indian Institute of Chemical Technology, Hyderabad 500 007, India
[d] Department of Medicinal Chemistry, National Institute of Pharmaceutical Education and Research (NIPER), Hyderabad 500 037, India

ARTICLE INFO

Article history:
Received 21 May 2014
Revised 13 July 2014
Accepted 18 July 2014
Available online xxxx

Keywords:
Podophyllotoxin
Benzimidazole
Cytotoxicity
Tubulin polymerization
Molecular docking

ABSTRACT

A series of new podophyllotoxin derivatives containing structural modifications at C-7, C-8, and C-9 were synthesized and evaluated for their cytotoxic activity against three human cancer cell lines. All the synthesized compounds showed significant growth inhibition with GI_{50} values in micromolar levels while some of the compounds were several times more potent against MCF-7 and HeLa cell lines than MIAPACA cell line. Three compounds (**12a**, **12d** and **12e**) emerged as potent compounds with broad spectrum of cytotoxic activity against all the tested cell lines with GI_{50} values in the range of 0.01–2.1 μM. These compounds induce microtubule depolymerization and arrests cells at the G2/M phase of the cell cycle. Moreover, compounds **12d** and **12e** disrupted microtubule network and accumulated tubulin in the soluble fraction in a similar manner to their parent podophyllotoxin scaffold. In addition, structure activity relationship studies within the series were also discussed. Molecular docking studies of these compounds into the colchicine-binding site of tubulin, revealed possible mode of inhibition by these compounds.

1. Introduction

Podophyllotoxin **1**, the main component of *Podophyllum* resin, has long been used as cathartic, antirheumatic, antiviral and antitumor agent.[1] Inspite of its initial potential as an anticancer agent, its high toxicity and severe adverse effects[2] has limited its application as a drug in cancer chemotherapy, making this cyclolignan a lead compound for drug design in the search for improved pharmacological profiles. Extensive efforts on structural modification of podophyllotoxin has led to the clinical introduction of semisynthetic derivatives like etoposide (**2**), teniposide (**3**) and etopophos (**4**) for the treatment of a variety of malignancies including lung and testicular carcinoma, lymphoma, nonlymphocytic leukemia, etc.[3–6] Despite their wide clinical applications, there are several limitations such as poor water solubility, development of drug resistance, metabolic inactivation, and toxic effects which has inspired to further search for new effective antitumor agents based on this scaffold (Fig. 1).[7]

Interestingly, podophyllotoxin and these semisynthetic derivatives, substantially differ in their mechanism of action. Podophyllotoxin and its related 4′-methoxy congeners inhibits tubulin polymerization through interaction at the colchicine binding site, preventing the formation of the spindle and arresting cell division in metaphase.[8,9] Whereas, 4′-demethylepipodophyllotoxin derivatives (etoposide and its analogues) primarily inhibit DNA topoisomerase II, induce a premitotic blockade in late S stage of the cell cycle.[10] Etoposide binds to and stabilizes the DNA–protein complex preventing relegation of the double-stranded breaks.[11]

The core structural features like transfused γ-lactone, fused dioxole ring, and the almost orthogonal free-rotating 3,4,5-trimethoxyphenyl fragment are considered essential for antitubulin activity of podophyllotoxin derivatives.[12] Although, literature survey revealed that podophyllic aldehyde (**5**) and its analogues that lack trans-lactone D-ring, showed significant cytotoxicity against various tumor cell lines confirming that the γ-lactone ring is not an essential feature for cytotoxicity and antimitotic activity, whereas the presence of an electrophilic function at C-7/ C-9 seemed to be important for the cytotoxicity for this type of derivatives.[13,14] Structural activity relationship studies of podophyllic aldehyde revealed that the C-8 neighbouring area is favourable for generating structural modification and diversification, with the aim of adding extra fragments that would increase receptor site occupation and could enhance the affinity and selectivity of interaction of podophyllotoxin related lignans with the tubulin protein.[15]

* Corresponding author. Tel.: +91 40 27193157; fax: +91 40 27193189.
E-mail address: ahmedkamal@iict.res.in (A. Kamal).

http://dx.doi.org/10.1016/j.bmc.2014.07.031
0968-0896/

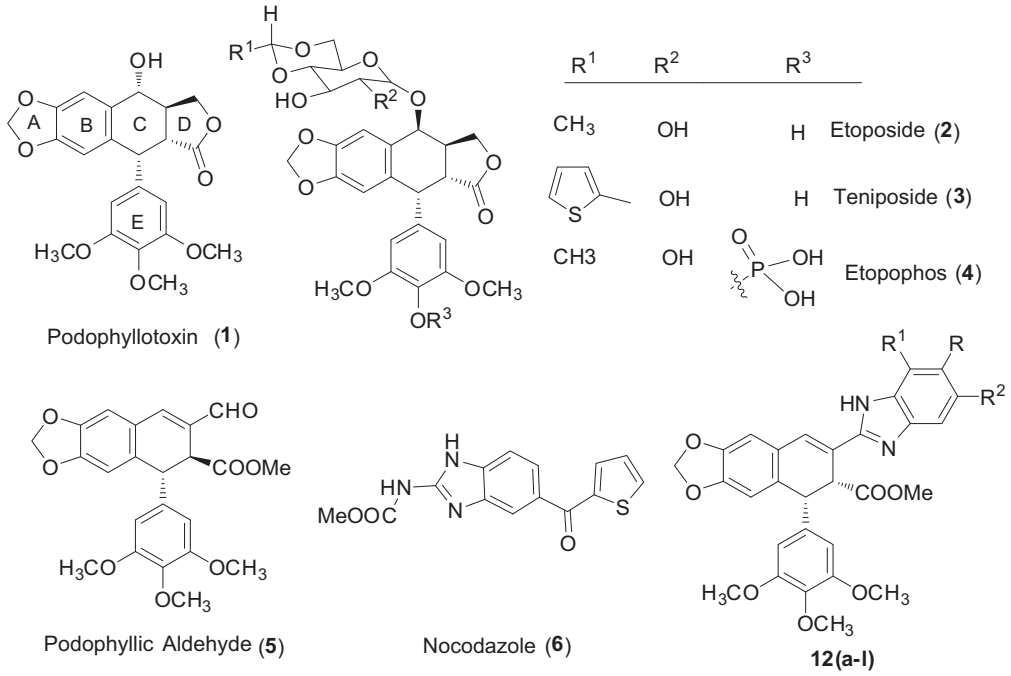

Figure 1. Structures of podophyllotoxin (**1**), etoposide (**2**), teniposide (**3**), etopophos (**4**), podophyllic aldehyde (**5**), nocodazole (**6**) and target molecules **12(a–l)**.

Recently, there has been increasing interest in molecules containing benzimidazole rings due to their broad range of pharmacological activities such as antimicrobial,[16] anti-HIV,[17] anti inflammatory,[18] antiulcer,[19] antihypertensive[20] and anticancer.[21] Benzimidazoles can easily interact with biomolecules of the living systems due to their structural similarity with naturally occurring compounds such as indole and purine nuclei, that are present in a number of fundamental cellular components as well as bioactive compounds. Benzimidazole substituted derivatives like nocodazole (**6**) are also known as inhibitors of tubulin polymerization and are useful for inhibiting cell proliferation for the treatment of cancer.[22]

In view of these observations and in continuation to our previous efforts that were aimed to find newer podophyllotoxin based molecules with potential anticancer activities,[23–25] it was considered worthwhile to design and synthesize new hybrids that comprises of both podophyllotoxin as well as benzimidazole ring systems as promising anticancer agents. Therefore, we synthesized a series of new podophyllotoxins with linkage to a benzimidazole sharing at C-8 and α-configuration at C-8[1] position. All the synthesized derivatives were evaluated for their antiproliferative activity against certain human cancer cell lines.

2. Chemistry

As illustrated in Scheme 1, these compounds (**12a–l**) were synthesized using podophyllotoxin (**1**) as the starting material.[13] Briefly, intermediate **9** was prepared from **1** through successive oxidation with pyridinium dichromate (PDC) and subsequent acid-catalyzed methanolysis to give the D-ring opened compound (**9**). Stereoselective reduction of the 7-carbonyl group of compound **9** afforded the dihydroxy compound **10**. The Swerns oxidation of the dihydroxy-ester (**10**) led to the oxidation of the hydroxyl group at C-9 and the elimination of the hydroxyl group at C-7 to afford the unsaturated aldehyde **11**. Finally the target compounds **12**(**a–l**) were synthesized by reacting the unsaturated aldehyde with appropriate o-phenylenediamine in presence of sodium metabisulfate. The structures of all target compounds were confirmed by ^{1}H NMR, ^{13}C NMR, MS and HRMS.

3. Pharmacology

3.1. In vitro antiproliferative activity

All the synthesized podophyllotoxin-benzimidazole conjugates **12(a–l)** were evaluated for their antiproliferative activity against the three tumor cell lines: MIAPACA (pancreatic), HeLa (cervical) and MCF-7 (breast carcinoma) employing SRB assay. Podophyllotoxin and etoposide were used as the reference standards and the he results obtained are shown in Table 1. It is observed that, the majority of the tested compounds displayed significant growth inhibition on MCF-7 and HeLa cancer cell lines as compared with MIAPACA cell line. With the exception of compounds **12f**, **12g**, **12k**, the tested compounds showed significant cytotoxicity, with GI_{50} values in sub micromolar level, while some of the compounds **12a**, **12b**, **12d**, **12e**, **12h** and **12i** exhibited potent growth inhibition values in the nanomolar range close to, or even better than, those of the podophyllotoxin, etoposide and nocodazole on certain cell lines. However, compound **12d** exhibited enhanced activity than etoposide and podophyllotoxin against all the three cancer cell lines with GI_{50} values in the range of 0.01–0.54 μM.

Based on the cytotoxicity data, the structure activity relationship (SAR) for these new podophyllotoxin congeners (**12a–l**) was examined. The introduction of substituents at 4-position of the benzimidazole ring such as flouro, chloro and bromo improved the activities as exemplified by analogs **12b**, **12c** and **12d**. However, electron releasing groups like methoxy and methyl substituent at 4-position of the benzimidazole ring produced compounds **12e** and **12f** with moderate cytotoxic activities. Moreover, the presence of different disubstitutions on the phenyl ring of the benzimidazole, such as 3,4-dimethyl (**12h**), 3,5-dichloro (**12i**), 3-flouro-4-chloro (**12j**) and 3-bromo-5-triflouromethyl (**12k**) groups are selectively active on MCF-7 cell lines with GI_{50} values in the range of 0.16–2.1 μM and showed moderate activity towards the other cell lines. It is also observed that the extension of ring A to the naphthalene (**12l**) showed selective cytotoxicity on MCF-7 cell lines in nanomolar range. Finally, it is worth highlighting that the introduction of relatively large and bulky substituent like

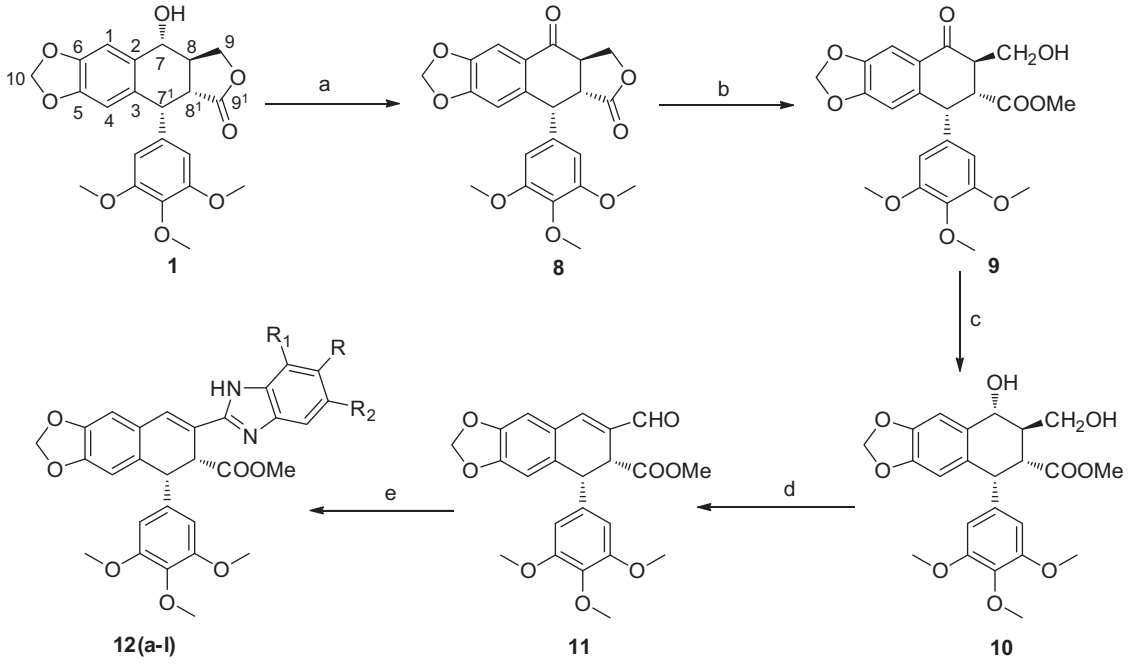

12a ; R = R^1 = R^2 = H
12b ; R = F, R^1 = R^2 = H
12c ; R = Cl, R^1 = R^2 = H
12d ; R = Br, R^1 = R^2 = H
12e ; R = OMe, R^1 = R^2 = H
12f ; R = Me, R^1 = R^2 = H
12g ; R = CF_3, R^1 = R^2 = H
12h ; R = R^2 = Me, R^1 = H
12i ; R = R^2 = Cl, R^1 = H
12j ; R = F, R^1 = Cl, R^2 = H
12k ; R = H, R^1 = Br, R^2 = CF_3
12l ; R^1 = H, R = R^2 = Condensed benzene ring

Scheme 1. Reagents and conditions: (a) PDC/CH_2Cl_2, rt, 2 h; (b) H_2SO_4/CH_3OH, reflux, 2 h; (c) $NaBH_4$/CH_3OH, rt, 0.5 h; (d) $(COCl)_2$, DMSO, Et_3N, CH_2Cl_2, −55 °C, 0.5 h to 0 °C, 1 h; (e) corresponding *o*-phenylenediamines, sodium metabisulfate, EtOH, reflux, 2–5 h.

Table 1
Antiproliferative activity ([a]GI_{50} μM) of compounds **12(a–l)**

Compound	MIAPACA[b]	MCF-7[c]	HeLa[d]
11	0.73 ± 0.021	0.91 ± 0.01	0.69 ± 0.03
12a	1.2 ± 0.7	0.2 ± 0.01	0.2 ± 0.1
12b	3.9 ± 4.4	0.02 ± 0.01	4.3 ± 6.4
12c	1.3 ± 0.1	2.09 ± 0.2	2.16 ± 1.4
12d	<0.01	0.54 ± 0.4	0.21 ± 0.21
12e	1.6 ± 0.5	2.1 ± 0.3	1.04 ± 0.01
12f	18.1 ± 2.4	3.07 ± 0.4	2.8 ± 0.4
12g	NA	4.8 ± 0.8	5.08 ± 0.5
12h	1.5 ± 2.5	0.16 ± 0.1	3.6 ± 0.6
12i	3.2 ± 2.6	0.58 ± 0.06	19.7 ± 3.4
12j	NA	2.3 ± 0.9	24.2 ± 0.9
12k	3.1 ± 0.2	2.1 ± 0.6	6.4 ± 0.6
12l	2.56 ± 0.2	1.2 ± 1.1	3.8 ± 1.5
Podophyllotoxin	0.51 ± 0.1	0.31 ± 0.19	0.74 ± 0.23
Etoposide	1.1 ± 0.32	0.25 ± 0.21	0.62 ± 0.17
Nacodazole	0.95 ± 0.013	0.94 ± 0.02	0.81 ± 0.01

NA = not active.
[a] 50% Growth inhibition and the values are mean of three independent experiments.
[b] Pancreatic cancer.
[c] Breast cancer.
[d] Cervix cancer.

benzimidazole ring at position C-9, these compounds showed significant growth inhibition on three tumor cell lines, despite the lack of the γ-lactone ring, which is generally considered as an essential structural feature for the cytotoxicity of this class of compounds. The significant growth inhibitory activity exhibited by promising compounds like **12a**, **12d** and **12e** prompted us to evaluate their detailed biological effects.

3.2. Inhibition of in vitro tubulin polymerization

To examine whether these compounds bind to tubulin and inhibit its polymerization, representative compounds **12a**, **12d** and **12e** were subjected to evaluation by tubulin assembly assay. Podophyllotoxin was also evaluated by this assay as a positive control. To test this, varying concentrations of compounds **12a**, **12d** and **12e** were incubated with tubulin protein. The result indicated that, compound **12d** significantly decreased tubulin assembly with IC_{50} value 0.86 μM and is comparable to IC_{50} of podophyllotoxin (**1**). In contrast, **12a** and **12e** decreased tubulin polymerization with an IC_{50} of 1.29 μM and 0.91 μM, respectively. These results show the rational relationship between the inhibition of tubulin polymerization and the corresponding cytotoxic activities. The order of inhibition of tubulin polymerization was **1** > **12d** > **12e** > **12a** (Table 2)

3.3. Antimitotic effects of active compounds

As the inhibition of tubulin polymerization has been implicated in G2/M phase of the cell cycle arrest in various cancer cell lines,[26]

Table 2
Antitubulin activity of compounds **12a**, **12d** and **12e**

S. No	Compound	IC_{50} (μM)
1	**12a**	1.29
2	**12d**	0.86
3	**12e**	0.91
4	**1**	0.83

Effect of compounds on tubulin polymerization. IC_{50} values for **12a**, **12d** and **12e** were determined from the tubulin polymerization assays.

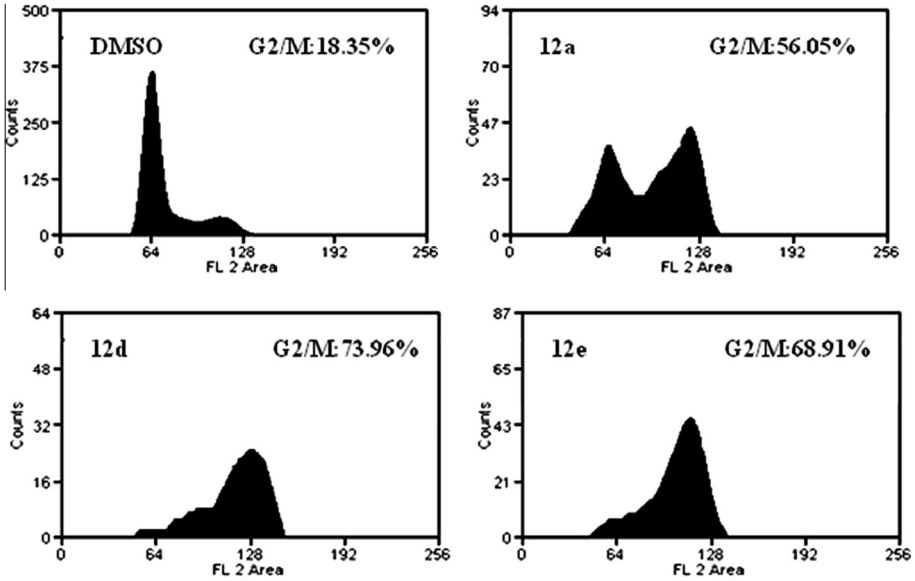

Figure 2. Anti-mitotic effects of **12a**, **12d** and **12e** by FACS analysis: induction of cell cycle G2/M arrest by compounds **12a**, **12d** and **12e**. HeLa cells were harvested after treatment at 5 μM and for 24 h. Untreated cells and DMSO treated cells served as controls. The percentage of cells in each phase of cell cycle was quantified by flow cytometry.

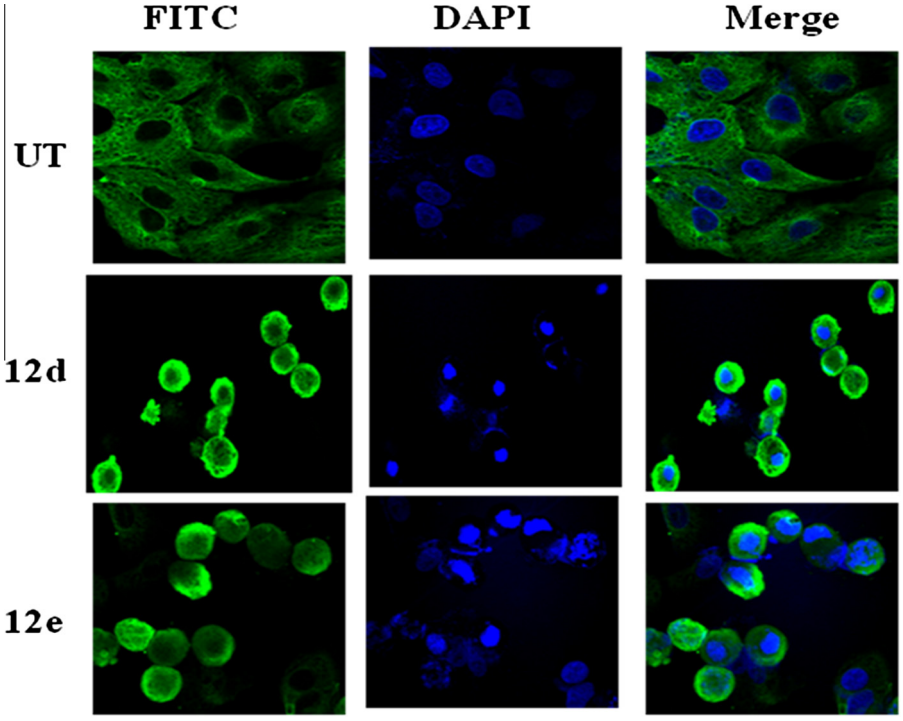

Figure 3. Effect of **12d** and **12e** on microtubules and nuclear condensation HeLa cells were independently treated with **12d** and **12e** at 5 μM concentrations for 24 h. Following the termination of experiment, cells were fixed and stained for tubulin. DAPI was used as counter stain. The merged images of cells stained for tubulin and DAPI are represented.

the effect of compounds **12a**, **12d** and **12e** on the cell cycle progression of the HeLa cells was determined by flow cytometric analysis. HeLa cells were treated with 5 μM concentration of compounds for 24 h. DMSO treated cells showed predominant G1 phase, with 18.35% of cells in G2/M. In contrast, **12e** treated cells showed 68.91% cells in G2/M phase, which increased to 73.96% on treatment by **12d** treatments. However, **12a** manifested 56.05% of cells in G2/M phase. Overall, these results suggest that these compounds efficiently stall cells at G2/M phase (Fig. 2).

3.4. Effects of 12d and 12e on cellular microtubules and nuclear morphology

Microtubule depolymerizing drugs cause improper chromosome separation by inhibiting the organization of the mitotic spindle, and predominantly arrest chromosomes in metaphase of mitosis.[27] Therefore to identify the effect of compounds **12d** and **12e** on tubulin cytoskeleton by immunohistochemistry, human breast cancer HeLa cells were treated with the compounds at 5 μM concentrations for 24 h and later the cells were stained with

antitubulin antibody. It is observed that the tubulin network was severely disrupted in cells treated with **12d** and **12e**. DAPI was employed to stain nucleus. In contrast, cells treated with DMSO demonstrated a normal and intact tubulin organization (Fig. 3).

3.5. Distribution of soluble versus polymerized tubulin in cell

Microtubules are in dynamic equilibrium with tubulin dimers as tubulin is polymerized into microtubules and depolymerized as free tubulin and this dynamic equilibrium is targeted by microtubule disrupting agents.[28] Therefore, in order to assess the effect of **12d** and **12e** on the cellular microtubules, we analyzed the levels of soluble and polymerized fractions of tubulin in HeLa cells by treatment with compounds **12d** and **12e** for 24 h. In DMSO treated HeLa cells, there was relatively even distribution of the tubulin was found among both the fractions. In cells treated with podophyllotoxin, a tubulin depolymerizing agent, a remarkable shift was obtained in tubulin protein, most of the tubulin protein was found in soluble fraction. Similarly, **12d** treated cells showed a predominant accumulation of tubulin in soluble fraction. In comparison, paclitaxel (tubulin polymerizing agent) contained tubulin in the polymerized fraction. Therefore, these results suggest that **12d** and **12e** function as microtubule-destabilizing agent (Fig. 4).

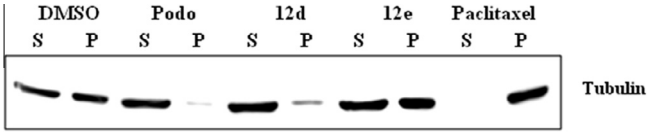

Figure 4. Distribution of tubulin in polymerized vs soluble fractions as analyzed by immunoblotting in **12d** and **12e** treated HeLa cells: the cells were treated with 5 μM of **12d**, **12e** and podophyllotoxin for 24 h. Tubulin was detected by Immunoblot analysis.

Table 3
Glide scores of compounds **12a**, **12d** and **12e** docked into the colchicine binding site of tubulin-podophyllotoxin crystal structure (PDB code: 1SA1)

Compound	Glide score
12a	−9.173
12d	−10.503
12e	−9.044
Podophyllotoxin	−9.199

3.6. Molecular docking

Molecular docking studies were performed using Maestro 9.5 (Schrodinger package)[29] to validate whether the synthesized compounds have comparable binding mode to that of podophyllotoxin for α,β-tubulin. Compounds **12a**, **12d** and **12e** exhibiting the most potent cytotoxicity in all the cell lines tested were docked into the colchicine binding site of tubulin-podophyllotoxin crystal structure (PDB code: 1SA1). As depicted in Figure 5, the compounds interacted with the colchicine binding site formed from the αSer178, αThr179, βCys241, βLeu242, βLeu248, βAla250, βLys254, βLeu255, βAsn258, βMet259, βAla316, βAla317, βLys352, βThr353 and βIle378 residues in a similar manner to that of podophyllotoxin. As in the case of podophyllotoxin, the benzodioxole binds into the hydrophobic pocket formed by βMet259, βAla316, and βLys352; whereas the trimethoxyphenyl ring inserted quasiaxially in the hydrophobic cavity formed by βCys241, βLeu242, βLeu248, βAla250, βLys254, βLeu255, βAsn258, βAla317 and βThr353. The hydrogen bonding exhibited by the C ring –OH group with αThr179 in podophyllotoxin is compensated by that of –NH of the benzimidazole ring in our conjugates. Further, one of the oxygens of the trimethoxyphenyl ring formed H-bonding with βCys241. All these interactions together contribute to the hypothesis that the synthesized compounds exhibit efficient binding into the colchicine

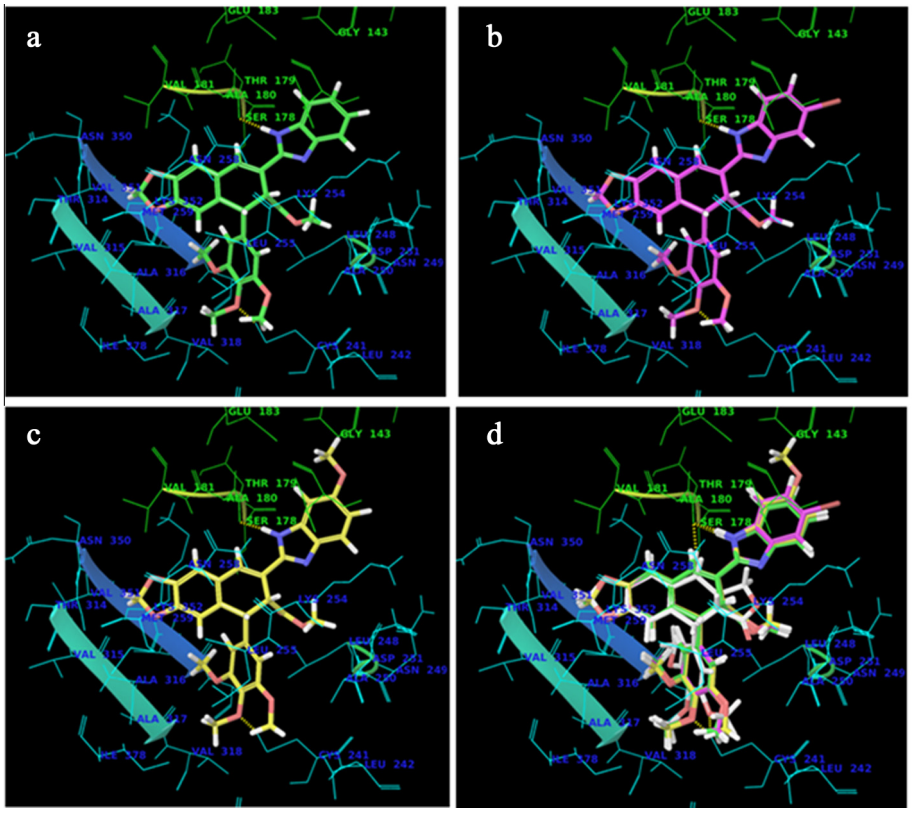

Figure 5. Molecular docking of (a) **12a** (lime green), (b)**12d** (magenta), (c) **12e** (yellow) into the colchicine binding site of tubulin (PDB code: 1SA1). (d) All molecules overlaid with podophyllotoxin (in white). α-Chain is shown in green and β-chain in blue.

binding site on tubulin and thus, the ensuing antimitotic activity as in the case of podophyllotoxin (Table 3).

4. Conclusion

A series of lactone ring opened podophyllotoxin congeners (**12a**–**l**) with modifications at C-7, C-8, C-9 were synthesized and tested for their cytotoxic activity. These compounds have retained the antineoplastic cytotoxicity despite the lack of the γ-lactone ring, which is generally considered as an essential structural feature for the cytotoxicity of the podophyllotoxin class of compounds. Three compounds **12a**, **12d** and **12e** emerged as lead molecules with broad spectrum of anticancer activity against all the tested tumor cell lines and inhibited the tubulin polymerization, comparable to that of podophyllotoxin. The flow cytometric analysis indicated that these compounds induced G2/M cell cycle arrest in HeLa treated cells and inhibited tubulin assembly, disrupted microtubules, increased the amount of tubulin in soluble fraction as other antitubulin agents. The molecular modeling study on tubulin demonstrated that these molecules bind well with the tubulin and are involved in a series of interactions with the protein. Thus this study reveals that incorporating certain structural fragments that are bioactive by themselves, such as benzimidazole moiety at the C-9 position of podophyllotoxin scaffold could lead to better anticancer agents.

5. Experimental section

All chemicals and reagents were obtained from Aldrich (Sigma–Aldrich, St. Louis, MO, USA), Lancaster (Alfa Aesar, Johnson Matthey Company, Ward Hill, MA, USA) and were used without further purification. Reactions were monitored by TLC, performed on silica gel glass plates containing 60 F-254, and visualization on TLC was achieved by UV light or iodine indicator. ^{1}H and ^{13}C NMR spectra were recorded on INOVA (400 MHz) or Gemini Varian-VXR-unity (200 MHz) or Bruker UXNMR/XWIN-NMR (300 MHz) instruments using $CDCl_3$ or DMSO as solvents. Chemical shifts (δ) are reported in ppm downfield from internal TMS standard. ESI spectra were recorded on Micro mass, Quattro LC using ESI^+ software with capillary voltage 3.98 kV and ESI mode positive ion trap detector. Melting points were determined with an Electrothermal melting point apparatus, and are uncorrected. HRMS spectra were recorded on a Q-TOF6510 spectrograph.

5.1. (5a*R*,8a*R*,9*R*)-9-(3,4,5-trimethoxyphenyl)-5a,6,8a,9-tetrahydrofuro [3′,4′:6,7] naphtha [2,3-*d*][1,3]dioxole-5,8-dione (8)

PDC (2.0 g, 5.34 mmol) was added to a solution of podophyllotoxin (**1**, 2 g, 4.83 mmol) in dry CH_2Cl_2 at 0 °C and was stirred at rt for 3 h. The reaction mixture was quenched with and dilute with CH_2Cl_2. The organic layer was dried over anhydrous Na_2SO_4 and concentrated in vacuo. The resulting product was purified by column chromatography to afford pure compound **8** in 1.84 g (92%) yield. Physical and spectroscopic data were identical to those reported. Mp = 177−179 °C [literature, 174 °C].[30] $[\alpha]_D^{25.6}$ −71.39 ± 57.97 (*c* 0.91 mg/mL, $CHCl_3$).

5.2. (5*R*,6*R*,7*R*)-methyl 7-(hydroxymethyl)-8-oxo-5-(3,4,5-trimethoxyphenyl)-5,6,7,8-tetrahydronaphtho[2,3-*d*][1,3]dioxole-6-carboxylate (9)

To a solution of compound **8** (1.5 g, 3.64 mmol) in methanol was added 4 equivalents of H_2SO_4 at 0 °C. The reaction mixture was stirred at reflux for 5 h. Then the solvent was removed in vacuo, and quenched with sodium bicarbonate, diluted with EtOAc. The organic layer was dried over Na_2SO_4 and evaporated. The residue was purified by column chromatography to afford pure product in 0.73 g, 89% isolated yield of **9** based upon recovered **8**; mp. 137–139 °C. $[\alpha]_D^{26.6}$ −89.34 ± 30.34 (*c* 1.23 mg/mL, $CHCl_3$). ^{1}H NMR (300 MHz, $CDCl_3$) δ 7.28 (s, 1H), 7.09 (s, 1H), 6.36 (s, 1H), 6.28 (s, 2H), 5.95 (s, 2H), 4.78 (d, *J* = 8.1 Hz, 1H), 4.05–4.28 (m, 2H), 3.81 (s, 3H), 3.78 (s, 6H), 3.55 (s, 3H), 3.01 (dd, *J* = 12.0, 5.6 Hz, 1H), 2.39 (m, 2H). MS (ESI): *m*/*z* 468 $[M+Na]^+$.

5.3. (5*R*,6*R*,7*R*,8*R*)-methyl 8-hydroxy-7-(hydroxymethyl)-5-(3,4,5-trimethoxyphenyl)-5,6,7,8-tetrahydronaphtho[2,3-*d*][1,3]dioxole-6-carboxylate (10)

To a stirred solution of compound **9** (1.0 g, 2.25 mmol) in methanol (20 mL) was added $NaBH_4$ (100 mg, 2.7 mmol) at 0 °C and the reaction was stirred for 2 h at rt. The reaction mixture was then quenched with saturated aq NH_4Cl and diluted with EtOAc (150 mL). The organic layer was dried over anhydrous Na_2SO_4 and concentrated under vacuum. The resulting crude product was purified by column chromatography to afford pure product in 66% yield. Mp. 145–149 °C. $[\alpha]_D^{26.6}$ −114.34 ± 26.59 (*c* 1.09 mg/mL, $CHCl_3$). ^{1}H NMR (500 MHz, $CDCl_3$) δ 7.29 (s, 1H), 7.08 (s, 1H), 6.38 (s, 1H), 6.22 (s, 2H), 5.92 (d, *J* = 0.8 Hz, 2H), 4.78 (d, *J* = 8.1 Hz, 1H), 4.31 (d, *J* = 5.6 Hz, 1H), 4.05 (dd, *J* = 10.3, 3.6 Hz, 1H), 3.82 (s, 3H), 3.76 (s, 6H), 3.56 (s, 3H), 3.01 (dd, *J* = 12.0, 5.6 Hz, 1H), 2.39 (m, 2H). MS (ESI): *m*/*z* 469 $[M+Na]^+$. HRMS (ESI) calcd for $C_{23}H_{26}O_9Na$ [M+Na]+ 469.14690; found: 469.14708.

5.4. (5*R*,6*R*)-methyl 7-formyl-5-(3,4,5-trimethoxyphenyl)-5,6-dihydronaphtho[2,3-*d*][1,3]dioxole-6-carboxylate (11)

To a stirred solution of oxalyl chloride (0.24 mL, 2.7 mmol) in dry CH_2C1_2 (5 mL) at −55 °C, was added DMSO (0.4 mL, 5.6 mmol) dropwise. After 5 min, a solution of 400 mg (0.90 mmol) of compound **10** in 3 mL of dry CH_2C1_2 was slowly added. The mixture was stirred at the same temperature for 30 min, and then triethylamine (1.27 mL, 9.10 mmol) was added dropwise. Then, the reaction mixture was warmed to 0 °C and stirred for 1 h, quenched with water and extracted with CH_2C1_2. The organic layer was dried over Na_2SO_4, concentrated in vacuo. The obtained residue was purified by column chromatography to afford compound **11** in 58% yield. Mp: 154–156 °C. $[\alpha]_D^{25.7}$ 129.57 ± 38.86 (*c* 0.94 mg/mL, $CHCl_3$). ^{1}H NMR (300 MHz, $CDCl_3$) δ 9.61 (s, 1H), 7.37 (s, 1H), 6.89 (s, 1H), 6.62 (s, 1H), 6.46 (s, 2H), 5.95 (d, *J* = 1.3 Hz, 1H), 5.94 (d, *J* = 1.3 Hz, 1H), 4.41 (d, *J* = 7.1 Hz, 1H), 3.98 (d, *J* = 7.4 Hz, 1H), 3.87 (s, 3H), 3.81 (s, 6H), 3.50 (s, 3H). MS (ESI): *m*/*z* 427 $[M+H]^+$. HRMS (ESI) calcd for $C_{23}H_{23}O_8$ [M+H]+ 427.13874; found: 427.13872.

5.5. General preparation of compounds 12(a–l)

To a mixture of compound **11** (0.46 mmol) and appropriate *o*-phenylenediamines (0.46 mmol) in ethanol was added a solution of $Na_2S_2O_5$ (770 mg, 4 mmol) in H_2O (1.6 mL). The resulting mixture was stirred at reflux for 4 h. after completion of reaction; the solution was evaporated under reduced pressure to remove ethanol, and partitioned between EtOAc and water. The organic layer was dried over Na_2SO_4, and concentrated in vacuo. The crude product was purified by column chromatography using EtOAc/hexane as eluant to afford pure compounds **12(a–l)** in good yields.

5.5.1. ((5*R*,6*R*)-Methyl 7-(1*H*-benzo[*d*]imidazol-2-yl)-5-(3,4,5-trimethoxyphenyl)-5,6-dihydronaphtho[2,3-*d*][1,3]dioxole-6-carboxylate) (12a)

This compound **12a** was prepared by method described in Section 5.5 employing (5*R*,6*R*)-methyl 7-formyl-5-(3,4,5-trime-

thoxyphenyl)-5,6-dihydronaphtho[2,3-*d*][1,3]dioxole-6-carboxylate (**11**, 200 mg, 0.46 mmol) and o-phenylenediamine (48 mg, 0.46 mmol) to affords **12a** as off white solid 184 mg, in 76% yield. Mp: 161–164 °C; $[\alpha]_D^{25}$ 276 ± 32.07 (*c* 0.99 mg/mL, $CHCl_3$). ^{1}H NMR (300 MHz, $CDCl_3$) δ 7.51 (dd, *J* = 6.0, 3.1 Hz, 2H), 7.27 (s, 1H), 7.20 (dd, *J* = 6.0, 3.1 Hz, 2H), 6.83(s, 1H), 6.61 (s, 1H), 6.20 (s, 2H), 5.95 (d, *J* = 1.3 Hz, 1H), 5.94 (d, *J* = 1.3 Hz, 1H), 4.57 (d, *J* = 4.3 Hz, 1H), 4.38 (d, *J* = 4.4 Hz, 1H), 3.87 (s, 3H), 3.79 (s, 6H), 3.48 (s, 3H). ^{13}C NMR (75 MHz, $CDCl_3$) δ 172.2, 153.3, 150.9, 148.1, 146.3, 144.1, 139.3, 138.0, 137.2, 134.8, 129.1, 126.9, 122.9, 114.3, 109.8, 108.5, 106.5, 101.2, 61.0, 56.0, 51.9, 48.7, 48.1. MS (ESI): *m*/*z* 515 $[M+H]^+$. HRMS (ESI) calcd for $C_{29}H_{27}O_7N_2$ [M+H]+ 515.18128; found: 515.18064.

5.5.2. ((5*R*,6*R*)-Methyl 7-(6-fluoro-1*H*-benzo[d]imidazol-2-yl)-5-(3,4,5-trimethoxyphenyl)-5,6-dihydronaphtho[2,3-*d*][1,3]dioxole-6-carboxylate) (12b)

This compound **12b** was prepared by method described in Section 5.5 employing (5*R*,6*R*)-methyl 7-formyl-5-(3,4,5-trimethoxyphenyl)-5,6-dihydronaphtho[2,3-*d*][1,3]dioxole-6-carboxylate (**11**, 200 mg, 0.46 mmol) and 4-flouro-1,2-phenylenediamine (58 mg, 0.46 mmol) to affords **12a** as off white solid 176 mg, in 70% yield. Mp: 245–248 °C; $[\alpha]_D^{25.1}$ 198 ± 65.01 (*c* 0.87 mg/mL, $CHCl_3$). ^{1}H NMR (300 MHz, $CDCl_3$) δ 7.39–7.48 (m, 2H), 7.21 (s, 1H), 6.91–7.02 (m, 2H), 6.61 (s, 1H), 6.29 (s, 2H), 5.99 (s, 2H), 4.60 (d, *J* = 4.3 Hz, 1H), 4.00 (d, *J* = 4.4 Hz, 1H), 3.87 (s, 3H), 3.80 (s, 6H), 3.46 (s, 3H). ^{13}C NMR (75 MHz, $CDCl_3$) δ 172.1, 157.9, 153.3, 151.7, 148.1, 146.9, 144.1, 141.2, 138.2, 137.6, 135.1, 128.8, 126.8, 119.1, 110.7, 109.5, 108.2, 107.8, 101.8, 101.4, 60.8, 56.3, 52.1, 47.9, 45.7. MS (ESI): *m*/*z* 533 $[M+H]^+$. HRMS (ESI) calcd for $C_{29}H_{26}O_7N_2F$ [M+H]+ 533.17186; found: 533.17099.

5.5.3. ((5*R*,6*R*)-Methyl 7-(6-chloro-1*H*-benzo[*d*]imidazol-2-yl)-5-(3,4,5-trimethoxyphenyl)-5,6-dihydronaphtho[2,3-*d*][1,3]dioxole-6-carboxylate) (12c)

This compound **12c** was prepared by method described in Section 5.5 employing (5*R*,6*R*)-methyl 7-formyl-5-(3,4,5-trimethoxyphenyl)-5,6-dihydronaphtho[2,3-*d*][1,3]dioxole-6-carboxylate (**11**, 200 mg, 0.46 mmol) and 4-chloro-1,2-phenylenediamine (65 mg, 0.46 mmol) to affords **12c** as off white solid 170 mg, in 66% yield. Mp: 165–169 °C; $[\alpha]_D^{26.6}$ 116.73 ± 35.64 (*c* 1.40 mg/mL, $CHCl_3$). ^{1}H NMR (300 MHz, $CDCl_3$) δ 7.89 (s, 1H), 7.48 (d, *J* = 7.1 Hz, 1H), 7.29 (d, *J* = 7.3 Hz, 2H), 6.91 (s, 1H), 6.76 (s, 1H), 6.28 (s, 2H), 5.95 (s, 2H), 4.69 (d, *J* = 4.3 Hz, 1H), 4.05 (d, *J* = 4.5 Hz, 1H), 3.80 (s, 3H), 3.76 (s, 6H), 3.48 (s, 3H). ^{13}C NMR (75 MHz, $CDCl_3$) δ 172.8, 153.9, 151.6, 148.0, 146.4, 139.3, 138.6, 138.1, 137.3, 134.9, 129.2, 128.8, 126.6, 124.6, 118.1, 111.5, 109.8, 108.8, 106.7, 101.3, 60.9, 56.1, 52.2, 48.8, 47.9. MS (ESI): *m*/*z* 549 $[M+H]^+$. HRMS (ESI) calcd for $C_{29}H_{26}O_7N_2Cl$ [M+H]+ 549.14231; found: 549.14188.

5.5.4. ((5*R*,6*R*)-Methyl 7-(6-bromo-1*H*-benzo[*d*]imidazol-2-yl)-5-(3,4,5-trimethoxyphenyl)-5,6-dihydronaphtho[2,3-*d*][1,3]dioxole-6-carboxylate) (12d)

This compound **12d** was prepared by method described in Section 5.5 employing (5*R*,6*R*)-methyl 7-formyl-5-(3,4,5-trimethoxyphenyl)-5,6-dihydronaphtho[2,3-*d*][1,3]dioxole-6-carboxylate (**11**, 200 mg, 0.46 mmol) and 4-bromo-1,2-phenylenediamine (86 mg, 0.46 mmol) to affords **12d** as off white solid 188 mg, in 67% yield. Mp: 231–235 °C; $[\alpha]_D^{26.6}$ 127.14 ± 84.03 (*c* 0.78 mg/mL, $CHCl_3$). ^{1}H NMR (500 MHz, $CDCl_3$) δ 7.79 (s, 1H), 7.46–7.51 (m, 1H), 7.43 (d, *J* = 8.0 Hz, 1H), 7.20 (s, 1H), 6.91 (s, 1H), 6.62 (s, 1H), 6.27 (s, 2H), 6.05 (s, 2H), 4.61 (d, *J* = 4.7 Hz, 1H), 4.01–4.07 (m, 1H), 3.89 (s, 3H), 3.81 (s, 6H), 3.48 (s, 3H). ^{13}C NMR (75 MHz, $CDCl_3$) δ 172.9, 154.0, 151.6, 148.1, 146.6, 139.9, 138.5, 137.9, 137.4, 135.0, 129.3, 126.6, 125.8, 119.1, 115.6, 112.3, 109.9, 108.6, 106.5, 101.2, 60.7, 56.3, 52.1, 48.9, 47.6. MS (ESI): *m*/*z* 593 $[M+H]^+$. HRMS (ESI) calcd for [M+H]+ 593.09228; found: 593.09193.

5.5.5. ((5*R*,6*R*)-Methyl 7-(6-methoxy-1*H*-benzo[*d*]imidazol-2-yl)-5-(3,4,5-trimethoxyphenyl)-5,6-dihydronaphtho[2,3-*d*][1,3]dioxole-6-carboxylate) (12e)

This compound **12e** was prepared by method described in Section 5.5 employing (5*R*,6*R*)-methyl 7-formyl-5-(3,4,5-trimethoxyphenyl)-5,6-dihydronaphtho[2,3-*d*][1,3]dioxole-6-carboxylate (**11**, 200 mg, 0.46 mmol) and 4-methoxy-1,2-phenylenediamine (64 mg, 0.46 mmol) to affords **12e** as off white solid 172 mg, in 67% yield. Mp: 249–251 °C; $[\alpha]_D^{26.6}$ 31.84 ± 20.96 (*c* 1.19 mg/mL, $CHCl_3$). ^{1}H NMR (300 MHz, $CDCl_3$) δ 7.36 (d, *J* = 8.8 Hz, 1H), 7.29 (S, 1H), 7.23 (s, 1H), 6.96 (d, *J* = 8.7 Hz, 1H), 6.87 (s, 1H), 6.55 (s, 1H), 6.35 (s, 2H), 5.97 (d, *J* = 3.7 Hz, 2H), 4.68 (d, *J* = 3.9 Hz, 1H), 3.99 (d, *J* = 4.4 Hz, 1H), 3.80 (s, 3H), 3.76 (s, 3H), 3.73 (s, 6H), 3.44 (s, 3H). ^{13}C NMR (75 MHz, $CDCl_3$) δ 173.0, 156.5, 154.1, 151.3, 148.2, 146.5, 139.3, 138.4, 137.5, 136.9, 134.9, 129.3, 126.6, 118.8, 112.2, 109.9, 108.6, 106.5, 101.2, 99.3, 60.7, 56.3, 55.9, 52.1, 48.9, 47.6. MS (ESI): *m*/*z* 545 $[M+H]^+$; HRMS (ESI) calcd for $C_{30}H_{29}O_8N_2$ [M+H]+ 545.19240; found: 545.19226.

5.5.6. ((5*R*,6*R*)-Methyl 7-(6-methyl-1*H*-benzo[*d*]imidazol-2-yl)-5-(3,4,5-trimethoxyphenyl)-5,6-dihydronaphtho[2,3-*d*][1,3]dioxole-6-carboxylate) (12f)

This compound **12f** was prepared by method described in Section 5.5 employing (5*R*,6*R*)-methyl 7-formyl-5-(3,4,5-trimethoxyphenyl)-5,6-dihydronaphtho[2,3-*d*][1,3]dioxole-6-carboxylate (**11**, 200 mg, 0.46 mmol) and 4-methyl-1,2-phenylenediamine (56 mg, 0.46 mmol) to affords **12f** as off white solid 158 mg, in 64% yield. Mp: 164–166 °C; $[\alpha]_D^{26.6}$ 14.22 ± 83.26 (*c* 0.90 mg/mL, $CHCl_3$). ^{1}H NMR (500 MHz, $CDCl_3$) δ 7.59 (d, *J* = 7.41 Hz, 1H), 7.46 (s, 1H), 6.99 (d, *J* = 7.3 Hz, 1H), 6.88 (s, 1H), 6.58 (s, 1H), 6.36 (s, 2H), 5.95 (d, *J* = 1.3 Hz, 1H), 5.94 (d, *J* = 1.3 Hz, 1H), 4.61 (d, *J* = 3.7 Hz, 1H), 4.25–4.21 (m, 1H), 3.89 (s, 3H), 3.85 (s, 6H), 3.49 (s, 3H), 2.36 (s, 3H). ^{13}C NMR (75 MHz, $CDCl_3$) δ 173.6, 153.0, 151.0, 148.1, 146.9, 144.1, 139.4, 138.0, 137.3, 135.1, 128.8, 126.8, 121.9, 117.9, 114.1, 109.6, 108.2, 107.7, 101.3, 60.6, 52.8, 52.1, 47.6, 46.2, 21.6. MS (ESI): *m*/*z* 529 $[M+H]^+$. HRMS (ESI) calcd for $C_{30}H_{29}O_7N_2$ [M+H]+ 529.19693; found: 529.19517.

5.5.7. ((5*R*,6*R*)-Methyl 7-(6-(trifluoromethyl)-1*H*-benzo[*d*]imidazol-2-yl)-5-(3,4,5-trimethoxyphenyl)-5,6-dihydronaphtho[2,3-*d*][1,3]dioxole-6-carboxylate) (12g)

This compound **12g** was prepared by method described in Section 5.5 employing (5*R*,6*R*)-methyl 7-formyl-5-(3,4,5-trimethoxyphenyl)-5,6-dihydronaphtho[2,3-*d*][1,3]dioxole-6-carboxylate (**11**, 200 mg, 0.46 mmol) and 4-triflouromethyl-1,2-phenylenediamine (81 mg, 0.46 mmol) to affords **12g** as off white solid 164 mg, in 60% yield. Mp: 149–153 °C; $[\alpha]_D^{26.1}$ 95.06 ± 39.89 (*c* 1.54 mg/mL, $CHCl_3$). ^{1}H NMR (300 MHz, $CDCl_3$) δ 7.90 (d, *J* = 8.9 Hz, 1H), 7.78 (s, 1H), 7.36 (d, *J* = 8.8 Hz, 1H), 7.29 (s, 1H), 6.71 (s, 1H), 6.52 (s, 1H), 6.35 (s, 2H), 5.97 (d, *J* = 3.7 Hz, 2H), 4.68–4.73 (m, 1H), 3.97 (d, *J* = 4.4 Hz, 1H), 3.80 (s, 3H), 3.76 (s, 6H), 3.53 (s, 3H). ^{13}C NMR (75 MHz, $CDCl_3$) δ 173.0, 153.9, 151.8, 148.2, 146.4, 139.0, 137.7, 137.2, 135.1, 134.4, 129.2, 128.3, 126.5, 124.3, 119.6, 118.8, 112.3, 109.8, 108.7, 106.6, 101.1, 60.8, 56.2, 52.0, 48.4, 47.3. MS (ESI): *m*/*z* 583 $[M+H]^+$. HRMS (ESI) calcd for $C_{30}H_{26}O_7N_2F_3$ [M+H]+ 583.16866; found: 583.16893.

5.5.8. ((5*R*,6*R*)-Methyl 7-(5,6-dimethyl-1*H*-benzo[*d*]imidazol-2-yl)-5-(3,4,5-trimethoxyphenyl)-5,6-dihydronaphtho[2,3-*d*][1,3]dioxole-6-carboxylate) (12h)

This compound **12h** was prepared by method described in Section 5.5 employing (5*R*,6*R*)-methyl 7-formyl-5-(3,4,5-trimethoxyphenyl)-5,6-dihydronaphtho[2,3-*d*][1,3]dioxole-6-carboxylate (**11**,

200 mg, 0.46 mmol) and 4,5-dimethyl-1,2-phenylenediamine (63 mg, 0.46 mmol) to affords **12h** as off white solid 170 mg, in 66% yield. Mp: 156–160 °C; $[\alpha]_D^{26.6}$ 95.76 ± 28.92 (*c* 1.14 mg/mL, $CHCl_3$). ^1H NMR (300 MHz, $CDCl_3$) δ 7.48 (s, 1H), 7.46 (s, 1H), 7.22(s, 1H), 6.96 (s, 1H), 6.76 (s, 1H), 6.34 (s, 2H), 5.96 (s, 2H), 4.68 (d, *J* = 4.11 Hz, 1H), 4.09–4.14 (m, 1H), 3.79 (s, 3H), 3.76 (m, 6H), 3.56 (s, 3H), 2.38 (s, 6H). ^{13}C NMR (75 MHz, $CDCl_3$) δ 172.2, 153.3, 150.9, 148.1, 146.3, 144.1, 139.3, 138.7, 137.2, 134.8, 130.2, 129.1, 126.9, 115.7, 109.8,108.5, 106.5, 101.2, 61.0, 56.0, 51.9, 48.7, 48.1, 20.3. MS (ESI): *m*/*z* 543 $[M+H]^+$. HRMS (ESI) calcd for $C_{31}H_{31}O_7N_2$ [M+H]+ 543.21258; found: 543.21219.

5.5.9. ((5*R*,6*R*)-Methyl 7-(5,6-dichloro-1*H*-benzo[*d*]imidazol-2-yl)-5-(3,4,5-trimethoxyphenyl)-5,6-dihydronaphtho[2,3-*d*][1,3]dioxole-6-carboxylate) (12i)

This compound **12i** was prepared by method described in Section 5.5 employing (5*R*,6*R*)-methyl 7-formyl-5-(3,4,5-trimethoxyphenyl)-5,6-dihydronaphtho[2,3-*d*][1,3]dioxole-6-carboxylate (**11**, 200 mg, 0.46 mmol) and 4,5-dichloro-1,2-phenylenediamine (81 mg, 0.46 mmol) to affords **12i** as off white solid 154 mg, in 56.2% yield. Mp: 151–155 °C; $[\alpha]_D^{25.4}$ 29.50 ± 27.36 (*c* 1.01 mg/mL, $CHCl_3$). ^1H NMR (500 MHz, $CDCl_3$) δ 7.66 (s, 2H), 7.23 (s, 1H), 6.92 (s, 1H), 6.78 (s, 1H), 6.36 (s, 2H), 5.96 (d, *J* = 1.3 Hz), 5.94 (d, *J* = 1.3 Hz, 1H), 4.69 (d, *J* = 4.1 Hz, 1H), 4.01 (d, *J* = 4.1 Hz, 1H), 3.79 (s, 3H), 3.74 (s, 6H), 3.52 (s, 3H). ^{13}C NMR (75 MHz, $CDCl_3$) δ 169.2, 153.4, 151.1, 148.2, 146.1, 142.6, 139.6, 137.9, 135.2, 134.5, 129.3, 126.6, 123.2, 117.5, 115.7, 108.9, 107.2, 106.4, 101.4, 61.0, 56.1, 52.0, 48.4, 47.1. MS (ESI): *m*/*z* 583 $[M+H]^+$. HRMS (ESI) calcd for $C_{29}H_{25}O_7N_2Cl_2$ [M+H]+ 583.10333; found: 583.10369.

5.5.10. (5*R*,6*R*)-Methyl 7-(5-chloro-6-fluoro-1*H*-benzo[*d*]imidazol-2-yl)-5-(3,4,5-trimethoxyphenyl)-5,6-dihydronaphtho[2,3-*d*][1,3]dioxole-6-carboxylate (12j)

This compound **12j** was prepared by method described in Section 5.5 employing (5*R*,6*R*)-methyl 7-formyl-5-(3,4,5-trimethoxyphenyl)-5,6-dihydronaphtho[2,3-*d*][1,3]dioxole-6-carboxylate (**11**, 200 mg, 0.46 mmol) and 4-chloro-5-flouro-1,2-phenylenediamine (74 mg, 0.46 mmol) to affords **12j** as off white solid 81 mg, in 60% yield. Mp: 235–238 °C; $[\alpha]_D^{26.1}$ 62.72 ± 40.00 (*c* 1.02 mg/mL, $CHCl_3$). ^1H NMR (300 MHz, $CDCl_3$) δ 7.75 (s, 1H), 7.36 (s, 1H), 7.21(s, 1H), 6.96 (s, 1H), 6.75 (s, 1H), 6.29 (s, 2H), 5.95 (s, 2H), 4.68–4.77 (m, 1H), 4.08 (d, *J* = 3.7 Hz, 1H), 3.81 (s, 3H), 3.78 (s, 6H), 3.48 (s, 3H). ^{13}C NMR (126 MHz, $CDCl_3$) δ 166.2, 154.3, 150.6, 150.0, 146.4, 145.9, 139.3, 177.2, 134.7, 133.0, 128.7, 125.0, 121.1, 114.7, 108.8, 107.8, 105.5, 104.5, 103.1, 101.2, 60.8, 56.0, 51.9, 48.2, 46.8. MS (ESI): *m*/*z* 567 $[M+H]^+$. HRMS (ESI) calcd for $C_{29}H_{25}O_7N_2ClF$ [M+H]+ 567.13288; found: 567.13219.

5.5.11. (5*R*,6*R*)-Methyl 7-(7-bromo-5-(trifluoromethyl)-1*H*-benzo[*d*]imidazol-2-yl)-5-(3,4,5-trimethoxyphenyl)-5,6-dihydronaphtho[2,3-*d*][1,3]dioxole-6-carboxylate (12k)

This compound **12k** was prepared by method described in Section 5.5 employing (5*R*,6*R*)-methyl 7-formyl-5-(3,4,5-trimethoxyphenyl)-5,6-dihydronaphtho[2,3-*d*][1,3]dioxole-6-carboxylate (**11**, 200 mg, 0.46 mmol) and 3-bromo-5-trifluromethyl-1,2-phenylenediamine (116 mg, 0.46 mmol) to affords **12k** as off white solid 186 mg, in 59% yield. Mp: 191–193 °C; $[\alpha]_D^{26}$ 11.13 ± 89.23 (*c* 0.88 mg/mL, $CHCl_3$). ^1H NMR (300 MHz, $CDCl_3$) δ 7.71 (s, 1H), 7.65(S, 1H), 7.21 (s, 1H), 6.95 (s, 1H), 6.78 (s, 1H), 6.30 (s, 2H), 5.99 (s, 2H), 4.66 (d, *J* = 3.4 Hz, 1H), 4.08 (d, *J* = 3.7 Hz, 1H), 3.81 (s, 3H), 3.76 (s, 6H), 3.66 (s, 3H). ^{13}C NMR (75 MHz, $CDCl_3$) δ 172.8, 153.6, 152.0, 148.3, 146.5, 141.2, 139.3, 137.5, 137.2, 135.0, 129.3, 128.2, 126.6, 124.3, 119.6, 115.7, 114.1, 109.9, 108.6, 106.4, 101.0, 60.6, 56.3, 51.9, 48.8, 47.6. MS (ESI): *m*/*z* 661 $[M+H]^+$. HRMS (ESI) calcd for $C_{30}H_{25}O_7N_2BrF_3$ [M+H]+ 663.07794; found: 663.07853.

5.5.12. ((5*R*,6*R*)-Methyl 7-(1*H*-naphtho[2,3-*d*]imidazol-2-yl)-5-(3,4,5-trimethoxyphenyl)-5,6-dihydronaphtho[2,3-*d*][1,3]dioxole-6-carboxylate) (12l)

This compound **12l** was prepared by method described in Section 5.5 employing (5*R*,6*R*)-methyl 7-formyl-5-(3,4,5-trimethoxyphenyl)-5,6-dihydronaphtho[2,3-*d*][1,3]dioxole-6-carboxylate (**11**, 200 mg, 0.46 mmol) and 2,3-diaminonapthalene (73 mg, 0.46 mmol) to affords **12l** as off white solid 174 mg, in 66% yield. Mp: 247–249 °C; $[\alpha]_D^{26.6}$ 238.54 ± 69.47 (*c* 0.82 mg/mL, $CHCl_3$). ^1H NMR (300 MHz, $CDCl_3$) δ 7.86–7.90 (m, 2H), 7.69–7.81 (m, 4H), 7.19 (s, 1H), 6.92 (s, 1H), 6.69 (s, 1H), 6.34 (s, 2H), 5.95 (s, 2H), 4.68 (d, *J* = 4.1 Hz, 1H), 4.01 (d, *J* = 4.3 Hz, 1H), 3.83 (s, 3H), 3.79 (s, 6H), 3.51 (s, 3H). ^{13}C NMR (75 MHz, $CDCl_3$) δ 172.8, 153.1, 150.2, 148.8, 146.6, 144.2, 139.3, 137.3, 135.4, 134.8, 130.0, 129.1, 127.8, 127.3, 126.8, 112.7, 109.9, 108.8, 106.3, 101.1, 60.9, 55.9, 51.8, 48.8, 48.3. MS (ESI): *m*/*z* 565 $[M+H]^+$. HRMS (ESI) calcd for $C_{33}H_{29}O_7N_2$ [M+H]+ 565.19693; found: 565.19532.

5.6. Cell cultures, maintenance and antiproliferative evaluation

The cell lines, MIAPACA (pancreatic), MCF-7 (breast), HeLa (cervical) which were used in this study were procured from American Type Culture Collection (ATCC), United States. The synthesized test compounds were evaluated for their in vitro antiproliferative activity in these three human cancer cell lines. A protocol of 48 h continuous drug exposure was used, and a SRB cell proliferation assay was used to estimate cell viability or growth. All the cell lines were grown in Dulbecco's modified Eagle's medium (containing 10% FBS in a humidified atmosphere of 5% CO_2 at 37 °C). Cells were trypsinized when sub-confluent from T25 flasks/60 mm dishes and seeded in 96-well plates in 100 μL aliquots at plating densities depending on the doubling time of individual cell lines. The microtiter plates were incubated at 37 °C, 5% CO2, 95% air, and 100% relative humidity for 24 h prior to addition of experimental drugs and were incubated for 48 h with different doses (0.01, 0.1, 1, 100, 1000 μM) of prepared derivatives. After 48 h incubation at 37 °C, cell monolayers were fixed by the addition of 10% (wt/vol) cold trichloroacetic acid and incubated at 4 °C for 1 h and were then stained with 0.057% SRB dissolved in 1% acetic acid for 30 min at room temperature. Unbound SRB was washed with 1% acetic acid. The protein-bound dye was dissolved in 10 mM Tris base solution for OD determination at 510 nm using a microplate reader (Enspire, Perkin Elmer, USA). Using the seven absorbance measurements [time zero, (Tz), control growth, (C), and test growth in the presence of drug at the five concentration levels (Ti)], the percentage growth was calculated at each of the drug concentrations levels. Percentage growth inhibition was calculated as:

$[(Ti - Tz)/(C - Tz)] \times 100$ for concentrations for which Ti>/=Tz

$[(Ti - Tz)/Tz] \times 100$ for concentrations for which Ti<Tz.

Growth inhibition of 50% (GI_{50}) was calculated from $[(Ti-Tz)/(C - Tz)] \times 100 = 50$, which is the drug concentration resulting in a 50% reduction in the net protein increase (as measured by SRB staining) in control cells during the drug incubation.

5.7. Tubulin polymerization assay

An in vitro assay for monitoring the time-dependent polymerization of tubulin to microtubules was performed employing a fluorescence-based tubulin polymerization assay kit (BK011, Cytoskeleton, Inc.) according to the manufacturer's protocol. The reaction mixture in a final volume of 10 μL in PEM buffer (80 mM PIPES, 0.5 mM EGTA, 2 mM $MgCl_2$, pH 6.9) in 384 well plates contained 2 mg/mL bovine brain tubulin, 10 μM fluorescent reporter, 1 mM GTP in the presence or absence of test compounds at 37 °C. Tubulin polymerization was followed by monitoring the fluorescence enhancement due to the incorporation of a

fluorescence reporter into microtubules as polymerization proceeds. Fluorescence emission at 420 nm (excitation wavelength is 360 nm) was measured for 1 h at 1 min intervals in a multimode plate reader (Tecan M200). Podophyllotoxin was used as positive control under similar experimental conditions. To determine the IC_{50} values of the compounds against tubulin polymerization, the compounds were pre-incubated with tubulin at varying concentrations (1, 2, 3, 4 and 5 μM). Assays were performed under similar conditions as employed for polymerization assays as described above.

5.8. Analysis of cell cycle

Human cervical cancer cell line (HeLa) in 60 mm dishes were incubated for 24 h in the presence or absence of test compounds **12a**, **12d** and **12e** (5 μM). Cells were harvested with Trypsin-EDTA, fixed with ice-cold 70% ethanol at 4 °C for 30 min, ethanol was removed by centrifugation and cells were stained with 1 mL of DNA staining solution [0.2 mg of propidium iodide (PI), and 2 mg RNase A] for 30 min. The DNA contents of 20,000 events were measured by flow cytometer (BD FACSCanto II). Histograms were analyzed using FCS express 4 plus.

5.9. Immunohistochemistry of tubulin and analysis of nuclear morphology

HeLa cells were seeded on glass cover slip, incubated for 24 h in the presence or absence of test compounds **12d** and **12e** at a concentration of 5 μM. Cells grown on coverslips were fixed in 3.5% formaldehyde in phosphate-buffered saline (PBS) pH 7.4 for 10 min at room temperature. Cells were permeabilized for 6 min in PBS containing 0.5% Triton X-100 (Sigma) and 0.05% Tween-20 (Sigma). The permeabilized cells were blocked with 2% BSA (Sigma) in PBS for 1 h. Later, the cells were incubated with primary antibody for tubulin from (sigma) at (1:200) diluted in blocking solution for 4 h at room temperature. Subsequently the antibodies were removed and the cells were washed thrice with PBS. Cells were then incubated with FITC labeled anti-mouse secondary antibody (1:500) for 1 h at room temperature. Cells were washed thrice with PBS and mounted in medium containing DAPI. Images were captured using the Olympus confocal microscope and analyzed with Provision software.

5.10. Western blot analysis of soluble versus polymerized tubulin

HeLa cells were seeded in 12-well plates at 1×10^5 cells per well in complete growth medium. Following treatment of cells with respective compounds (**12d**, **12e**, podophyllotoxin and paclitaxel) for a duration of 24 h, cells were washed with PBS and subsequently soluble and insoluble tubulin fractions were collected. To collect the soluble tubulin fractions, cells were permeabilized with 200 μL of pre-warmed lysis buffer [80 mM Pipes-KOH (pH 6.8), 1 mM $MgCl_2$, 1 mM EGTA, 0.2% Triton X-100, 10% glycerol, 0.1% protease inhibitor cocktail (Sigma–Aldrich)] and incubated for 3 min at 30 °C. Lysis buffer was gently removed, and mixed with 100 μL of 3 × Laemmli's sample buffer (180 mM Tris–Cl pH 6.8, 6% SDS, 15% glycerol, 7.5% β-mercaptoethanol and 0.01% bromophenol blue). Samples were immediately heated to 95 °C for 3 min. To collect the insoluble tubulin fraction, 300 μL of 1 × Laemmli's sample buffer was added to the remaining cells in each well, and the samples were heated to 95 °C for 3 min. Equal volumes of samples were run on an SDS-10% polyacrylamide gel and were transferred to a nitrocellulose membrane employing semidry transfer at 50 mA for 1 h. Blots were probed with mouse anti-human α-tubulin diluted 1:2,000 mL (Sigma) and stained with rabbit anti-mouse secondary antibody coupled with horseradish peroxidase, diluted 1:5000 mL (Sigma). Bands were visualized using an enhanced Chemiluminescence protocol (Pierce) and radiographic film (Kodak).

5.11. Molecular docking

Molecular docking was performed using Maestro 9.5 (Schrodinger package). For the binding site preparation, the structure of tubulin in complex with podophyllotoxin (PDB: 1SA1) was downloaded from the RCSB Protein Data Bank (http://www.rcsb.org/pdb). The preparation was done using the Schrodinger's protein preparation tool (PPrep) followed by energy minimization using OPLS 2005 force field with Polak–Ribiere Conjugate Gradient (PRCG) algorithm. The ligands were built using the builder feature in Maestro and each structure was prepared for docking using Ligprep 2.7 followed by molecular mechanics energy minimization using Macromodel 10.1. These geometrically optimized structures were used for Glide (grid-based ligand docking with energetics) docking using the 'Extra Precision' (XP) mode of Glide 6.0. The receptor-grid files were generated with a van der Waals scaling 0.4 and grid volume of $10 \times 10 \times 10$ Å at the centroid of each predicted binding site. Upon completion of each docking calculation, 100 poses per ligand were generated and the best docked structure was chosen using a GlideScore (Gscore) function.

Acknowledgments

T.S.R is thankful to IICT-RMIT Research centre for the award of research fellowship. A.V.S and V.G.R are thankful to CSIR-New Delhi for the award of the fellowship. We also acknowledge CSIR for financial support under the 12th Five Year plan project 'Affordable Cancer Therapeutics (ACT)' (CSC0301).

References and notes

1. Liu, Y. Q.; Yang, L.; Tian, X. *Curr. Bioact. Compd.* **2007**, *3*, 37.
2. Imbert, T. F. *Biochimie* **1998**, *80*, 207.
3. Doyle, T. W. *Etoposide (VP-16) Current Status and New Developments*; Academic: New York, 1984.
4. Wang, Z. Q.; Kuo, Y. H.; Schnur, D.; Bowen, J. P.; Liu, S. Y.; Han, F. S.; Cheng, Y. C.; Lee, K. H. *J. Med. Chem.* **1990**, *33*, 2660.
5. Fields, S. J.; Igwemezie, L. N.; Kaul, S.; Schacter, L. P.; Schilder, R. J.; Litam, P. P.; Himpler, B. S.; Mcaleer, C.; Wright, J.; Barbhaiya, R. H.; Langer, C. J.; Odwyer, P. *Clin. Cancer Res.* **1995**, *1*, 105.
6. (a) Schacter, L. P.; Igwemezie, L. N.; Seyedsadr, M. *Cancer Chemother. Pharmacol.* **1994**, *34*, s58; (b) Budman, D. R. *Semin. Oncol.* **1996**, *23*, 8.
7. (a) Zhu, X. K.; Guan, J.; Tachibana, Y.; Bastow, K. F.; Cho, S. J.; Cheng, H. H.; Cheng, Y. C.; Gurwith, M.; Lee, K. H. *J. Med. Chem.* **1999**, *42*, 2441; (b) Xiao, Z.; Bastow, K. F.; Vance, J. R.; Sidwell, R. S.; Wang, H. K.; Chen, M. S.; Shi, Q.; Lee, K. H. *J. Med. Chem.* **2004**, *47*, 5140.
8. (a) Cortese, F.; Bhattacharyya, B.; Wolf, B. *J. Biol. Chem.* **1977**, *252*, 1134; (b) Haar, E.; Rosenkranz, H. S.; Hamel, E.; Day, B. W. *Bioorg. Med. Chem.* **1996**, *4*, 1659.
9. Islam, M. N.; Iskander, M. N. *Mini-Rev. Med. Chem.* **2004**, *4*, 1077.
10. Ross, W.; Rowe, T.; Glisson, B.; Yalowich, J.; Liu, L. *Cancer Res.* **1984**, *44*, 5857.
11. (a) Long, B. H.; Minocha, A. *Proc. Am. Assoc. Cancer Res.* **1983**, *24*, 1271; (b) Long, B. H.; Musial, S. T.; Brattain, M. G. *Biochemistry* **1984**, *23*, 1183.
12. (a) Damayanthi, Y.; Lown, J. W. *Curr. Med. Chem.* **1998**, *5*, 205; (b) Gordaliza, M.; Castro, M. A.; Miguel del Corral, J. M.; San Feliciano, A. *Curr. Pharm. Des.* **1811**, *2000*, 6.
13. (a) Gordaliza, M.; Castro, M. A.; Miguel del Corral, J. M.; Lopez-Vazquez, M. L.; Garcia, P. A.; San Feliciano, A.; Garcia-Gravalos, M. D.; Broughton, H. *Tetrahedron* **1997**, *53*, 15743; (b) Li, J.; Hua, H. M.; Tang, Y. B.; Zhang, S.; Ohkoshi, E.; Lee, K. H.; Xiao, Z. *Bioorg. Med. Chem. Lett.* **2012**, *22*, 4293.
14. Castro, M. A.; Miguel del Corral, J. M.; Gordaliza, M.; Garcia, P. A.; Gomez-Zurita, M. A.; Garcia-Gravalos, M. D.; de la Iglesia-Vicente, J.; Gajate, C.; An, F.; Mollinedo, F.; San Feliciano, A. *J. Med. Chem.* **2004**, *47*, 1214.
15. Castro, M. A.; Miguel del Corral, J. M.; Garcia, P. A.; Rojo, M. V.; de la Iglesia-Vicente, J.; Mollinedo, F.; Cuevas, C.; San Feliciano, A.; Castro, M. A.; Castro, M. A. *J. Med. Chem.* **2010**, *53*, 983.
16. Shingalapur, R. V.; Hosamani, K. M.; Keri, R. S. *Eur. J. Med. Chem.* **2009**, *44*, 4244.
17. Miller, J. F.; Turner, E. M.; Gudmundsson, K. S.; Jenkinson, S.; Splatenstein, A.; Thomson, M.; Wheelan, P. *Bioorg. Med. Chem. Lett.* **2010**, *20*, 2125.
18. (a) Achar, K. C. S.; Hosamani, K. M.; Seetharamareddy, H. R. *Eur. J. Med. Chem.* **2010**, *45*, 2048; (b) El-Nezhawy, A. O.; Biuomy, A. R.; Hassan, F. S.; Ismaiel, A. K.; Omar, H. A. *Bioorg. Med. Chem.* **2013**, *21*, 1661.

19. Nagata, K.; Satoh, H.; Iwahi, T.; Shimoyama, T.; Tamura, T. *Antimicrob. Agents Chemother.* **1993**, *37*, 769.
20. Xu, J. Y.; Zeng, Y.; Ran, Q.; Wei, Z.; Bi, Y.; He, Q. H.; Wang, Q. J.; Hu, S.; Zhang, J.; Tang, M. Y.; Hua, W. Y.; Wu, X. M. *Bioorg. Med. Chem. Lett.* **2007**, *17*, 2921.
21. (a) Luo, Y.; Xiao, F.; Qian, S.; Lu, W.; Yang, B. *Eur. J. Med. Chem.* **2011**, *46*, 417; (b) Hranjec, M.; Pavlovi, G.; Marjanovi, M.; Kralj, M.; Zamola, G. K. *Eur. J. Med. Chem.* **2010**, *45*, 2405; (c) Penning, T. D.; Zhu, G. D.; Gong, J.; Thomas, S.; Gandhi, V. B.; Liu, X.; Shi, Y.; Klinghofer, V.; Johnson, E. F.; Park, C.; Fry, E.; Donawho, C.; Frost, D.; Buchanan, G.; Bukofzer, G.; Rodriguez, L.; Bontcheva-Diaz, V.; Bouska, J.; Osterling, D. J.; Olson, A.; Marsh, K. C.; Luo, Y.; Giranda, V. *J. Med. Chem.* **2010**, *53*, 3142.
22. (a) Duanmu, C.; Shahrik, L. K.; Holly, H. H.; Hamel, E. *Cancer Res.* **1989**, *49*, 1344; (b) Vasquez, R. J.; Howell, B.; Yvon, A. M.; Wadsworth, P.; Cassimeris, L. *Mol. Biol. Cell* **1997**, *8*, 973.
23. Kamal, A.; Suresh, P.; Ramaiah, M. J.; Srinivasareddy, T.; Kapavarapu, R. K.; Rao, B. N.; Imthiajali, S.; Lakshminarayanreddy, T.; Pushpavalli, S. N. C. V. L.; Shankaraiah, N.; Pal-Bhadra, M. *Bioorg. Med. Chem.* **2013**, *21*, 5198.
24. Kamal, A.; Tamboli, J. R.; Nayak, V. L.; Adil, S. F.; Vishnuvardhan, M. V. P. S.; Ramakrishna, S. *Bioorg. Med. Chem.* **2014**, *22*, 2714.
25. Kamal, A.; Tamboli, J. R.; Nayak, V. L.; Adil, S. F.; Vishnuvardhan, M. V. P. S.; Ramakrishna, S. *Bioorg. Med. Chem. Lett.* **2013**, *23*, 273.
26. Kasibhatla, S.; Gourdeau, H.; Meerovitch, K.; Drewe, J.; Reddy, S.; Qiu, L.; Zhang, H.; Bergeron, F.; Bouffard, D.; Yang, Q.; Herich, J.; Lamothe, S.; Cai, S. X.; Tseng, B. *Mol. Cancer Ther.* **2004**, *3*, 1365.
27. Hastie, S. B. *Pharmacol. Ther.* **1991**, *51*, 377.
28. Reddy, M. A.; Jain, N.; Yada, D.; Kishore, C.; Vangala, J. R.; Reddy, P. S.; Addlagatta, A.; Kalivendi, S. V.; Sreedhar, B. *J. Med. Chem.* **2011**, *54*, 6751.
29. Schrödinger; LLC: New York, NY, 2012.
30. Miguel del Corral, J. M.; Gordaliza, M.; López, J. L.; del Olmo, E.; Castro, M. A.; Morales, L.; López, M. L. *Helv. Chim. Acta* **1995**, *78*, 1793.